



Biogenic Synthesis of Zinc Oxide Nanoparticles Using *Saponaria officinalis* L., Characterisation and Antibacterial Activities

Hamdi Kamçı¹, Hasan Ufuk Celebioğlu², Recep Taş^{3*}, Ebru Koroglu⁴

¹ Bartın Universtisy, Faculty of Science, Department of Biotechnology, Bartın, Turkey, (ORCID: 0000-0001-9255-2125), hkamci@bartin.edu.tr

² Bartın Universtisy, Faculty of Science, Department of Biotechnology, Bartın, Turkey, (ORCID: 0000-0001-7207-2730), hcelebioglu@bartin.edu.tr

^{3*} Bartın Universtisy, Faculty of Science, Department of Biotechnology, Bartın, Turkey, (ORCID: 0000-0002-3743-7770), rtas@bartin.edu.tr

⁴ Bartın Universtisy, Faculty of Science, Department of Biotechnology, Bartın, Turkey, (ORCID: 0000-0001-9357-4668), eburkoroglu@gmail.com

(First received 17 February 2022 and in final form 25 March 2022)

(DOI: 10.31590/ejosat.1075292)

ATIF/REFERENCE: Kamçı, H., Celebioğlu, H. U., Taş, R. & Koroglu, E. (2022). Biogenic Synthesis of Zinc Oxide Nanoparticles Using *Saponaria officinalis* L., Characterisation and Antibacterial Activities. *European Journal of Science and Technology*, (35), 227-234.

Abstract

The bioactivity exhibited by nanoparticles is of great interest by researchers worldwide. Phytogetic synthesis of zinc oxide nanoparticles (ZnO NPs) has been an environmentally friendly approach due to its low toxicity and biological potential. Today, ZnO NPs are frequently the subject of research due to their usability in many different fields such as biomedicine, water treatment, environmental improvement, and their applicability in the food industry and cosmetic products. It is known that ZnO produced by biosynthesis methods exhibits various nanostructures with antimicrobial, antioxidant, and anticancer properties. For this reason, studies on the antioxidant and antibacterial activity of ZnO NPs produced by green synthesis methods are increasing day by day. In this study, the biosynthesis of ZnO NPs was carried out by evaluating the root parts of the *Saponaria officinalis* plant with high polyphenol content used in the food industry, bread making, and soap making in the cosmetics sector. Nanoparticle characterizations were performed by UV-VIS absorption spectroscopy, FT-IR, XRD, and SEM analysis. These Green-ZnO NPs were shown to have antibacterial activity against the tested bacterial strains.

Keywords: Green synthesis, ZnO, Nanoparticles, *Saponaria officinalis*, Antibacterial activity.

Saponaria officinalis L. Kullanılarak Çinko Oksit Nanopartiküllerin Biyojenik Sentezi, Karakterizasyon ve Antibakteriyel Aktiviteler

Öz

Nanopartiküllerin sergilediği biyoaktivite, dünya çapındaki araştırmacılar tarafından büyük ilgi görmektedir. Çinko oksit nanoparçacıklarının (ZnO NP'ler) fitojenik sentezi, düşük toksisitesi ve biyolojik potansiyeli nedeniyle çevre dostu bir yaklaşım olmuştur. ZnO NP'ler günümüzde biyomedikal, su arıtma, çevre iyileştirme gibi çok farklı alanlarda kullanılabilirliği, bunun yanında gıda sektöründe ve kozmetik ürünlerde uygulanabilirliği nedeniyle çok sık araştırma konusu yapılmaktadır. Biyosentez yöntemleriyle üretilen ZnO'nun antimikrobiyal, antioksidan ve antikanser özelliklere sahip çeşitli nanoyapılar sergilediği bilinmektedir. Bu nedenle yeşil sentez yöntemleriyle üretilen ZnO NP'lerin antioksidan ve antibakteriyel aktivitesi üzerine yapılan çalışmalar her geçen gün artmaktadır. Bu çalışmada, gıda endüstrisinde, ekmek yapımında ve kozmetik sektöründe sabun yapımında kullanılan yüksek polifenol içeriğine sahip *Saponaria officinalis* bitkisinin kök kısımları değerlendirilerek ZnO NP'lerin biyosentezi gerçekleştirilmiştir. Sentezlenen Nanopartiküllerin karakterizasyonu UV-VIS absorpsiyon spektroskopisi, FT-IR, XRD ve SEM analizi ile gerçekleştirilmiştir. Bu Green-ZnO NP'lerinin test edilen bakteri suşlarına karşı antibakteriyel aktiviteye sahip olduğu gösterildi.

Anahtar Kelimeler: Yeşil sentez, ZnO, Nanopartiküller, *Saponaria officinalis*, Antibakteriyel aktivite.

* Corresponding Author: hkamci@bartin.edu.tr

1. Introduction

From the material science point of view nanoparticles are scalarly defined as (the commonly cited definition) particles with at least one of the dimensions measured in 1-100 nm range (Aitken, Creely, & Tran, 2004; Buzea, Pacheco, & Robbie, 2007; Linsinger, Roebben, Solans, & Ramsch, 2011). In the unit definition, the name nanoparticle refers to individual small single-unit materials that can be measured at the nanoscale. (Linsinger et al., 2011). Based on this information, the common denominator in the definition of nanomaterials is that the dimensions are limited to the nanoscale.

Concerning nanoparticles, the term “enhanced surface to volume ratio at the nanoscale” is usually misinterpreted. Proper terminology instead is the "specific surface area" (SSA) (Linsinger et al., 2011), which is rarely used. By simple reasoning on this correct term (SSA), we can conclude that a small decrease in the radius of any nanoparticle will lead to a large increase in the SSA score; i.e.; as we change the size of the nanoparticle by any small step, the specific surface area changes by a significant amount at the nanoscale (Guo, Xie, & Luo, 2014). Consequently the whole potential of the atoms making up a single nanoparticle will be more prominently reflected as nanoparticle size decreases due to higher SSA. A comparison between gold nanoparticles and gold nanodots may serve as an appropriate example at this point.

Metal oxide NPs (especially ZnO NPs) are utilised as antibacterial and antifungal agents in research, cosmetics, medicine and food industry. Main cause for special interest on zinc oxide nanocrystals, (i.e., zinc oxide nanoparticles) as antimicrobial agents might be attributed to its' non-toxicity to eukaryotic cells at therapeutic dosages. Metal oxides can be classified as inorganic-type antimicrobial agents and are better than antibiotics in terms of stability. (Padmavathy & Vijayaraghavan, 2008).

Since both some of the plant secondary metabolites and metal oxides possess antimicrobial activities, it is possible to combine the antimicrobial effects of both in the form of surface activated NPs coated with phytochemicals. Thus metal oxide nanoparticles synthesised through green route (Green-MetOx NPs) were reported to show dose-dependent bacteriostatic and bactericidal activities against a number of microorganisms tested (Elumalai & Velmurugan, 2015; Manzoor et al., 2016; Padmavathy & Vijayaraghavan, 2008; Zarrindokht Emami-Karvani, 2012).

An important aspect to mention during Green-NP synthesis is that, during synthesis, metal oxides generated would probably modify the bioactive compounds found in the biologic extracts (Bargebid & Khabnadideh, 2020). So to say, at the end of the green synthesis, both the nature of the metal oxide and the active antimicrobial agent may be.

Environmentally friendly nature and elimination of toxic byproducts during synthesis of Green-NPs are the first noticeable postulations of scientific reports. Considerable amounts among them note the use of various plants (with distinct therapeutic properties) as reducing and capping agents during NP synthesis. These NPs functionalized with plant extracts are foreseen as promising nano-therapeutic agents of the future (Vijayakumar, Mahadevan, Arulmozhi, Sriram, &

Praseetha, 2018; Wahab et al., 2011; Zarrindokht Emami-Karvani, 2012).

Compared to other metal oxide nanoparticles (CuO, TiO, FeO, etc.) ZnO has a prominent place, especially from an antimicrobial perspective, due to its nontoxic behavior on eukaryotic cells. The cost of synthesizing both green and chemical ZnO NPs is reasonable (Abdul Salam, Sivaraj, & Venckatesh, 2014; Bargebid & Khabnadideh, 2020; Chamjangali & Boroumand, 2013; Elumalai & Velmurugan, 2015; Yuvakkumar, Suresh, Nathanael, Sundrarajan, & Hong, 2014; Zarrindokht Emami-Karvani, 2012).

Widely applied procedure in both chemical synthesis and green synthesis methods is reduction of Zinc ions into Zinc-Oxide at high pH aqueous environment. In these methods two different sources of Zinc routinely used are Zinc Acetate ($Zn(CH_3CO_2)_2$) or Zinc Nitrate ($Zn(NO_3)_2$). Divergent methods distinguished from the above-stated aqueous synthesis are sol-gel synthesis (da Silva et al., 2020) and mechanochemical synthesis methods (Manzoor et al., 2016). In sol-gel synthesis method zinc nitrate mixed with gelatin is reduced to ZnO in the presence of KOH in aqueous, dried at 100°C and calcinated at 1000°C. Whereas in mechanochemical synthesis, zinc chloride ($ZnCl_2$) and sodium carbonate (Na_2CO_3) salts are thermally converted to ZnO and CO_2 at different temperatures. Scientific reports in which synthesis is made in aqueous media differ in terms of the use of different viscous agents (Anžlovar, Crnjak Orel, Kogej, & Žigon, 2012; Brayner et al., 2006) or condensing agents such as polyols (Krishnan & Pradeep, 2009), methanol (Cheng, Shi, Russell-Tanner, Zhang, & Samulski, 2006), or differ from one another in terms of annealing methods such as high pH (Krishnan & Pradeep, 2009) baking (Halbus, Horozov, & Paunov, 2020), calcination (Padmavathy & Vijayaraghavan, 2008) and autoclave at 70°C (Cheng et al., 2006). If we focus solely on green synthesis method we more frequently hit scientific papers that use zinc nitrate ($Zn(NO_3)_2$) than zinc acetate ($Zn(CH_3CO_2)_2$) as the zinc source. In these reports zinc ion reduction into zinc oxide precipitate usually catalyzed at around 60°C in continuous mixing conditions. The yielding zinc oxide precipitates are then annealed through calcination (Azizi et al., 2016; Hassan et al., 2018) or roasting (Selim, Azb, Ragab, & H. M. Abd El-Azim, 2020) at differing temperatures. Still some scientific reports diverge from the rest through usage of microwave radiation during the catalysis of reduction reaction in the presence of aqueous plant extracts (Sutradhar & Saha, 2015).

Because metal oxides are amphoteric, different charged metal oxides and phytochemicals are gradually stacked on top of each other as the nanoparticle develops. As we all know plant extracts hold plethora of bioactive chemicals with different ionized states with changing pH. And consequently, every NPs synthesized through green route possibly differ from one another on their particle size, activity, surface coatings, capping and hence structure, function and physical properties. For supporting this phenomenon we may refer to *Banerjee* who pointed out the effect of pH on properties of NP synthesized (Banerjee, Dubey, Gautam, Chattopadhyaya, & Sharma, 2019).

Besides its use as food additive (as emulsifier and foaming agent) *S. officinalis* plant parts have been used in folk medicine for numerous disease complications. And in research *S. officinalis* extracts are used as antioxidant, anticancer, antimicrobial agent (Chandra, Rawat, & Bhatt, 2021). Aerial

parts, seeds, and root parts of *S. officinalis* are used separately as sources of bioactive phytochemicals.

Aerial sections contain antimicrobials that are effective against many bacteria (Sengul et al., 2011). Important phytochemicals found in the above-ground parts of this plant can be summarized as flavonoids (which have potent antioxidant and antimicrobial activities), saponins, alkaloids, tannins, and vitamin C (Endonova, Antsupova, Zhamsaranova, & Lygdenov, 2015). Among these major phytochemicals sponging are ubiquitous agents found in seeds and root sections. *S. officinalis* seed sponins were shown to be effective protective agent in rats against ionizing radiation. (Kucukkurt et al., 2011). Root sections on the other hand are rich in saponins, and contain triterpene glycosides (Endonova et al., 2015), fatty acid (Slobodianiuk, Budniak, Marchyshyn, Kostyshyn, & Zakharchuk, 2021), tannin and phenolics (Jurado Gonzalez & Sørensen, 2020). The most abundant component found in root contents is stated as saponins (Sadowska et al., 2014; Tănase et al., 2021).

It is important to account for a specific property of the saponin of this plant. Unlike other detergents and surfactants saponins from *Saponaria* do not self-assemble into micellar structures (Tănase et al., 2021). That is, it is not an easy task to agglomerate metal oxides into NPs when saponins from *Saponaria* is used. Foam liberated at the start of synthesis may not die away even at the end of 20 hrs duration and may probably interfere with mixing of metal ions with the phytochemical content (Jurado Gonzalez & Sørensen, 2020). These two points will be touched later in discussion section.

2. Material and Method

2.1. Preparation of Plant Extracts

S. officinalis roots were collected from Bartın (Elevation: 9.574 Time Zone: Europe/Istanbul Latitude: 41° 38' 15.3672" N Longitude: 32° 20' 1.7196" E) at Ağdacı district. Collected roots were then thoroughly washed with distilled water and dry blotted on filter paper. Then, the dry root sections were first cut into small pieces and crushed into powder in a mortar. An aqueous crude bioactive phytochemical suspension was prepared on magnetic stirrer with 10 g of *S. officinalis* root powder in 100 ml of distilled water at room temperature. The plant tissue precipitate of the suspension was separated from the solution through filtration with filter paper. The resulting cloudy suspension-solution was stored at +4 °C in a dark glass bottle till use.

2.2. Synthesis of Zinc Oxide Nanoparticles

The green ZnO NP synthesis in this study was devised from modifying the chemical synthesis method used by Halbus et al., (Halbus et al., 2020). Zinc nitrate ($Zn(NO_3)_2 \cdot 6 H_2O$) was used as zinc ion source for synthesis of ZnO. In order to reduce zinc ions into zinc oxide with *S. officinalis* extracts, 0.1 M 100 ml $Zn(NO_3)_2 \cdot 6 H_2O$ solution was titrated dropwise with 50 ml of *S. officinalis* extract on magnetic stirrer. Development of ZnO was continued at 500 rpm stirring at room temperature for 24 hrs.

The usually accepted light to dark color transition in NP synthesis reaction mixture was also observed in our experimental setup. Developing color was prominently observable at the end of 15 min following addition of plant extract. At the end of 24 hrs resulting NPs yielded from the

reaction was sedimented through centrifugation at 8000 rpm for 15 minutes. The nanoparticles sedimented were separated from the supernatant and thoroughly washed with pure water twice. Whole sediment vacuum dried in the oven at 70°C for 12 hrs. In the final step of our Green-NP synthesis procedure NP annealing was performed in the furnace at 450°C for 3 hrs. Whole procedure in detail is schematized as flowchart in figure 1.

Annealed NPs were stored in tight closed test tubes at room temperature till characterizing and evaluation steps.

2.3. Characterization of zinc nanoparticles

UV-Visible absorbance spectrum (200-800 nm) analysis of the NPs' synthesized were made with THERMO Multiscaner-Go instrument. FTIR analysis were performed to diagnose available functional groups on the surface of nanocrystals. Fourier Transform Infrared Spectrophotometer analysis were performed with Shimadzu IRAffinity-1S. Particle morphology and size measurements were made with TESCAN, MAIA3 XM high-resolution scanning electron microscope. Crystallinity and particle size analysis of the synthesized ZnO NPs were evaluated through XRD analysis with Rigaku-Smartlab benchtop power X-Ray diffraction (XRD) instrument

2.4. Testing Anti-Bacterial Effects of Nanoparticles

Broth Micro-Dilution Assay was devised to test NPs' antibacterial activities (Brandt et al., 2010). Both gram-negative and gram-positive bacteria were used in the tests namely *Escherichia coli* and *Staphylococcus aureus*. Both bacteria were retrieved from -20°C stocks. After an initial refreshment in Nutrient Broth (NB) at 37°C, both bacteria were subcultured again in NB to achieve 0.5 McFarland Unit bacterial concentration for later use as the tester bacterial stock solution.

Antibacterial affect tests of the ZnO NPs were performed as follows. Whole test were performed with 200 µL microtiter plates. Each 200 µL well was first inoculated with 20 µL of test bacterial stock solution and aided with 160 µL NB media to support bacterial growth. And as the antimicrobial agent 20 µL solution of NP with varying concentrations of ZnO in it (in 50% DMSO) was added to each well.

Bacterial growths were detected with Thermo Scientific™ Multiskan GO Microplate Spectrophotometer instrument. For this optical density measurement values were recorded (as absorbance values as at 600 nm (OD_{600})) at culture start (zero hrs) and after 24 hrs of incubation at 37°C.

Evaluation antibacterial effects of NPs' were done through comparison of bacterial growths' optical density scores. During comparison of antibacterial effects, growth scores of positive control groups (that does contain any NPs but NB and DMSO) were referenced as full growth. Based on these measurements bacterial growth inhibitions were devised as percent depression against the full growth measure

2.5. Statistical Analysis

Statistical analysis of antibacterial tests were performed through one-way ANOVA or Students' t-test. Experimental score differences that fit into probabilities below 0.05 ($p < 0.05$) were considered statistically significant.

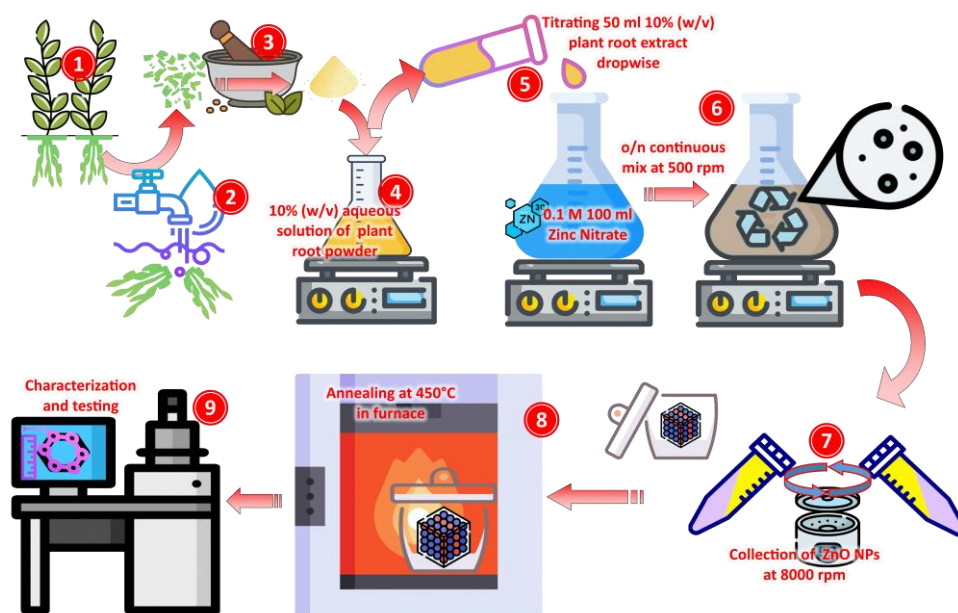


Figure 1. Schematics of Green ZnO NP synthesis employed in our work: Collection of *S. officinalis* roots and cleaning thoroughly with distilled water and blotting dry (1 & 2). Crushing the root sections into fine powder (3). Preparation of aqueous crude extract; 10 g powder/ 100 ml of distilled H₂O (4). Titrating 0.1 M 100 ml Zn(NO₃)₂·6H₂O solution with 50 ml of plant root extract and development of ZnO precipitate o/n at 500 rpm (5 & 6). Sedimentation of ZnO crystals in centrifuge (8000 rpm), collection and annealing at 450°C in furnace (7 & 8). Analysis diagnostics and tests of NPs synthesized (9). This Figure has been designed using the free resources from Flaticon.com

3. Results and Discussion

3.1. UV–Visible Absorption Spectrum Analysis

Synthesized ZnO nanoparticles were confirmed by the absorption maxima at the wavelength of 370 nm. The use of UV-Vis spectrophotometer stimulates the localized surface plasmon resonance in the metal, creating an electric field and resonance at a specific wavelength, which causes strong beam scattering at that wavelength. By this way, evaluation of spectrophotometric measurements; the scale used in different wavelengths colorly or colorimetrically is evaluated. *S. officinalis* extract provided reduction of zinc ion in ZnO NP complex, stimulation of surface plasmon resonance and consequently measurement was made in UV-Vis spectrophotometer (figure 2) (Nayak, Ashe, Rauta, Kumari, & Nayak, 2016).

3.2. Fourier-Transform Infrared Spectroscopy (FTIR) Analysis

FTIR spectrum analysis shows the relationship of absorption bands with chemical compounds in *S. officinalis* and ZnO NPs. The presence of functional groups of ZnO NPs are given in Figure 3 and the absorption peaks in the spectrum is seen at 3436 cm⁻¹, 1628 cm⁻¹, 1150 cm⁻¹, 1145 cm⁻¹, 875 cm⁻¹, 614 cm⁻¹ and 570 cm⁻¹. The wide peak observed at 3436 cm⁻¹ is due to O-H stress vibrations (Luo, Yang, Chen, Megharaj, & Naidu, 2016). Metal oxides form an absorption peak in the region between 600-400 cm⁻¹ due to inter-atomic vibrations. The characteristic peak corresponding to the Zn-O stress band showing ZnO formation was observed in the wave number of 570 cm⁻¹ (Anžlovar et al., 2012).

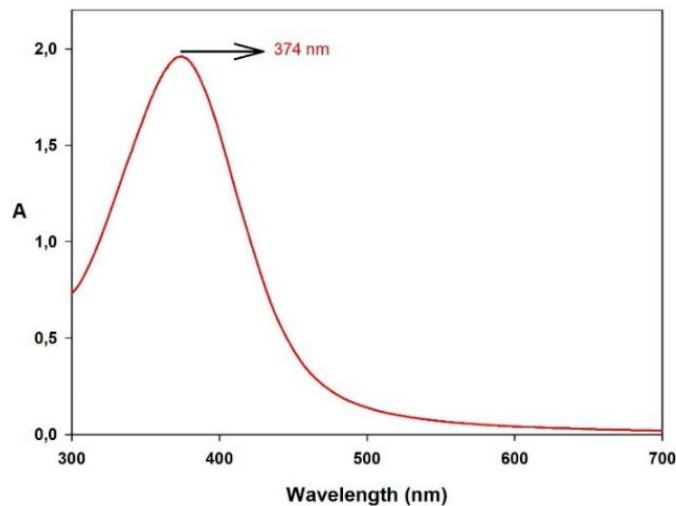


Figure 2. UV-visible spectrum (200-800 nm) absorbance scan of ZnO nanoparticles synthesised with *S. officinalis* root extracts

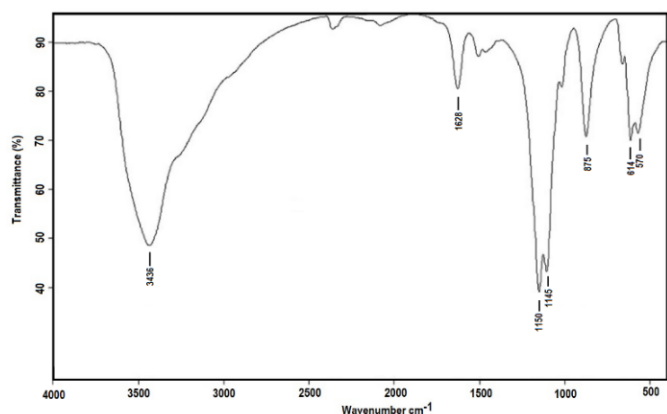


Figure 3. FTIR spectra of synthesised ZnO nanoparticles by *S. officinalis* extract. Synthesized ZnO nanoparticles were confirmed by the absorption maxima.

3.3. Scanning Electron Microscopy (SEM) Analysis of ZnO NPs

The structure, shape and size of ZnO NPs obtained by the green synthesis method were determined by SEM images. SEM images obtained with 50 kx, 100 kx and 200 kx magnifications show that the synthesized ZnO NPs have a spherical structure. The data obtained are similar to some studies (Chamjangali & Boroumand, 2013; Yuvakkumar et al., 2014). The optical performance of zinc nanoparticles may be affected by morphological form for real applications. SEM images (figure 4) of the *S. officinalis* mediated zinc nanoparticles established the presence of very small and uniformly spherical nanoparticles.

Chemical purity, elemental composition and stoichiometry of ZnO NPs were determined by EDX analysis. In EDX spectra shown in figure 4, it is seen that the peaks belong only to Zn and O. Therefore, it is confirmed that the synthesized ZnO NPs are of high purity. The stoichiometric mass percentage for Zn and O was 75.73219% and 24.26781%, respectively. It is seen that these results are consistent with the results of other studies in the literature (Abdul Salam et al., 2014)

3.4. XRD analysis

The XRD diffraction peaks of the ZnO NP samples obtained by the green synthesis method are shown in figure 5. Characteristic peaks of ZnO NPs at $2\theta = 31.80^\circ, 34.60^\circ, 36.24^\circ, 47.49^\circ, 56.65^\circ, 62.82^\circ, 68.17^\circ$, respectively (100), (002), (101), (102), (110), (103) and (112) planes. These data are matched with the JCPDS Data Card No: 65-3411 in the Joint Committee on Powder Diffraction Standards (JCPDS) database (Manzoor et al., 2016). In addition, since all the peaks seen in the graphic are characteristic peaks of ZnO, it confirms that they do not contain impurities. Crystal size measurement for synthesized ZnO NPs was calculated using the Debye-Scherrer equation (equation 1) (Aladpoosh & Montazer, 2015).

$$D = \frac{K\lambda}{\beta \cdot \cos\theta} \quad \text{Equation 1}$$

D: crystal size,
K: Debye Scherrer constant (0.94),
 λ : Cu-K α radiation (1.54 Å),

β : half length width of maximum peak (FWHM),
 θ : it is the Bragg angle value obtained from the 2θ value of the maximum peak in the XRD diffraction pattern.

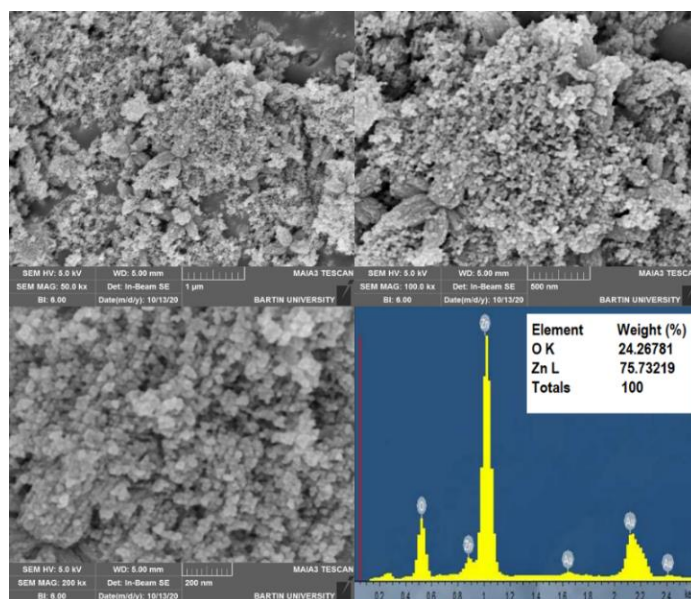


Figure 4. SEM images of ZnO NPs at different magnifications and EDX spectrum

The average crystal size of ZnO NPs was calculated to be approximately 14.83 nm according to the Debye-Scherrer formula. FWHM values are shown for each peak point determined to calculate the particle size in Table 1. The sharp bands of the Bragg peak confirm that the particles are in the nanoscale and are stabilized by the reducing agents contained in the plant root extract (Gnanadesigan et al., 2012).

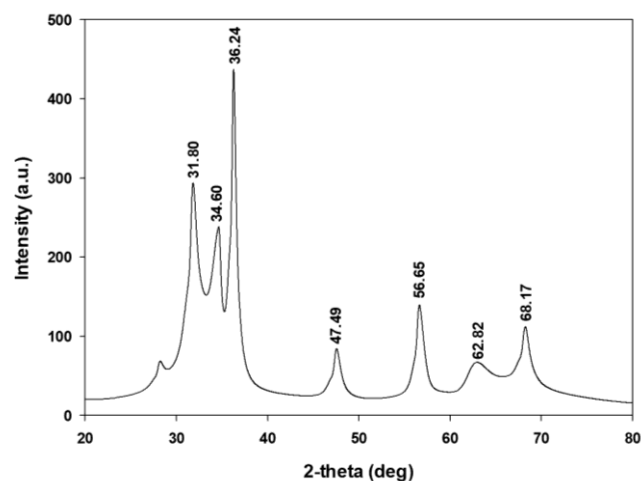


Figure 5. X-ray diffractogram of *S. officinalis* root extract-reduced ZnO NPs

3.5. Antibacterial Activity Tests

In the present study, we examined the anti-bacterial effects of ZnO nanoparticles synthesized using green synthesis with *S. officinalis* L. The results showed that this nanoparticle had slight anti-bacterial effect against very common bacterium *E. coli* (Figure 6A). Around 40% inhibition was observed in the bacterial growth of *E. coli* at 30 mM final ZnO NP concentration tested, which was the maximum used. Furthermore, MIC for *E. coli* was extrapolated as 73.0 ± 2.6 mM.

Table 1. Crystal sizes and peak values of ZnO NPs. XRD diffraction peaks of the ZnO NP samples obtained by the green synthesis

2 θ	h k l	FWHM	D (nm)
31.80	100	0.65	13.28
34.60	002	0.77	11.30
36.24	101	0.28	31.20
47.59	102	0.52	17.45
56.65	110	0.66	14.29
62.82	103	1.47	6.62
68.17	112	1.04	9.64

On the other hand, the nanoparticle greatly inhibited (90% decrease compared to control) the growth of *S. aureus* when used at maximum (30 mM) in our experimental setup. (Figure 6B). MIC for this bacterium was extrapolated as 33.5 ± 2.3 mM.

A previous study showed that bacteriostatic (MIC) activities of ZnO nanoparticles were found as 0.5 mg/mL (i.e. 6.14 mM) and 1.0 mg/mL (i.e. 12.3 mM) for *E. coli* and *S. aureus*, respectively (Zarrindokht Emami-Karvani, 2012). On the other hand, bactericidal (Minimum bactericidal concentration, MBC) effects were found as 16 mg/mL (196.6 mM) for *E. coli* and 8 (98.3 mM) mg/mL for *S. aureus*. These results also confirm that ZnO nanoparticles are more effective for *S. aureus* than *E. coli* (Zarrindokht Emami-Karvani, 2012).

Another study examined that ZnO nanoparticles that have the size of approximately 13 nm showed complete inhibition of *E. coli* growth at concentrations higher than 3.4 mM, but concentrations higher than 1 mM completely inhibited the growth of *S. aureus* (Reddy et al., 2007).

Augmented levels of ROS produced with MetOx is also considered Among the molecular mechanisms that nanoparticles show their anti-bacterial action. From the same respect in a number of scientific report on antibacterial effects of ZnO nanoparticles, researchers point out these ROS generated by NPs as the cause of antibacterial activity. (Brayner et al., 2006; Huang et al., 2008; Padmavathy & Vijayaraghavan, 2008; Sawai et al., 1998; Xia et al., 2008).

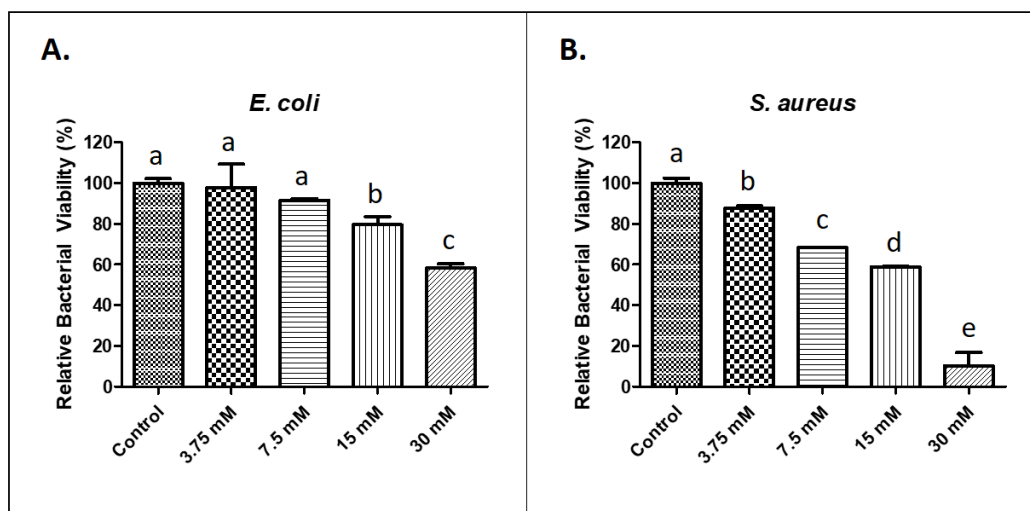


Figure 6. Anti-bacterial effects of ZnO nanoparticle synthesized with *S. officinalis* L. on (A) *Escherichia coli* and (B) *Staphylococcus aureus*. Different lower-case letters indicate the difference is statistically significant ($p < 0.05$) according to Tukey's multiple comparison test.

4. Conclusions and Recommendations

In this study we report green synthesis of ZnO NP with *S. officinalis* L. root extracts. At the end of synthesis, particles' UV-Visible absorption spectrum analysis revealed that particles generated are Zn nanoparticles.

SEM and XRD data suggests that NP synthesised showed almost spherical structures with the mean diameter of ~15 nm. We can state that *S. officinalis* L. root extracts are suitable for obtaining structurally and morphologically proper ZnO nanoparticles. In the FTIR spectrum graph with the measurement ranging from 3000 cm^{-1} to 1500 cm^{-1} , there was an apparent transmittance depression (approximately %22 depression) at 1628 cm^{-1} . This depression was attributed to polycyclic

aromatic compounds in literature where in our case this depression can be attributed to the saponins. Below 1500 cm^{-1} wavelength, in the fingerprint spectrum region, metal oxides are known to show their specific interatomic vibrations at $600\text{-}400 \text{ cm}^{-1}$ range. In this range, ZnO NPs are known for their Zn-O bond vibrations at 570 cm^{-1} wavelengths (Anžlovar et al., 2012), as is also seen in our FTIR data.

In this study, in vitro susceptibilities of both gram-positive and gram-negative bacterium against ZnO NPs synthesized from *S. officinalis* L. root extracts were determined by broth dilution method. Antibacterial activity of NPs may vary depending on microbial species. The most important growth inhibiting action of NP is thought to be exerted through the fusion of metal nanoparticles with negatively charged bacterial cell wall.

Combiend with ROS generation, such close interaction of NPs is assumed as the actual attack collapsing the bacterial cell wall and integrity. Considerable variation between cell wall structures of *E. coli* and *S. aureus*, can be regarded as the cause of diverging antibacterial action of the Green-ZnO NPs against gram negative and gram positive bacteria. The experimental results gathered in this report also supports the idea that ZnO NP can be regarded as alternative antibacterial agents with dual action modes as bactericidal or bacteriostatic.

When using green synthesis nomenclature, we implicitly imply that the reducing and capping power comes only from biological materials. But, the protein content from crude biological extracts may not be sufficient as capping agents (Elumalai & Velmurugan, 2015). At this stage, chemical capping may assist (Maruthupandy et al., 2017) green synthesis for better yields and results. From this respect, pure biochemical agents may also aid in our near future Green-NP synthesis.

5. Acknowledge

This study was partly supported by Bartin University.

References

- Abdul Salam, H., Sivaraj, R., & Venkatesh, R. (2014). Green synthesis and characterization of zinc oxide nanoparticles from *Ocimum basilicum* L. var. *purpurascens* Benth.-Lamiaceae leaf extract. *Materials Letters*, *131*, 16–18. <https://doi.org/10.1016/j.matlet.2014.05.033>
- Aitken, R. J., Creely, K. S., & Tran, C. L. (2004). Nanoparticles : An occupational hygiene review Prepared by the Institute of Occupational Medicine Nanoparticles : An occupational hygiene review. *Crown Copyright*, 7–18.
- Aladpoosh, R., & Montazer, M. (2015). The role of cellulosic chains of cotton in biosynthesis of ZnO nanorods producing multifunctional properties: Mechanism, characterizations and features. *Carbohydrate Polymers*, *126*, 122–129. <https://doi.org/10.1016/j.carbpol.2015.03.036>
- Anžlovar, A., Crnjak Orel, Z., Kogej, K., & Žigon, M. (2012). Polyol-mediated synthesis of zinc oxide nanorods and nanocomposites with poly(methyl methacrylate). *Journal of Nanomaterials*, *2012*. <https://doi.org/10.1155/2012/760872>
- Azizi, S., Mohamad, R., Bahadoran, A., Bayat, S., Rahim, R. A., Ariff, A., & Saad, W. Z. (2016). Effect of annealing temperature on antimicrobial and structural properties of bio-synthesized zinc oxide nanoparticles using flower extract of *Anchusa italica*. *Journal of Photochemistry and Photobiology B: Biology*, *161*, 441–449. <https://doi.org/10.1016/j.jphotobiol.2016.06.007>
- Banerjee, S., Dubey, S., Gautam, R. K., Chattopadhyaya, M. C., & Sharma, Y. C. (2019). Adsorption characteristics of alumina nanoparticles for the removal of hazardous dye, Orange G from aqueous solutions. *Arabian Journal of Chemistry*, *12*(8), 5339–5354. <https://doi.org/10.1016/j.arabjc.2016.12.016>
- Bargebid, R., & Khabnadideh, S. (2020). ZnO in ionic liquid under microwave irradiation: A novel medium for synthesis of phloroglucide derivatives as antimicrobial agents. *Indian Journal of Chemistry - Section B Organic and Medicinal Chemistry*, *59*(12), 1893–1902.
- Brandt, A. L., Castillo, A., Harris, K. B., Keeton, J. T., Hardin, M. D., & Taylor, T. M. (2010). Inhibition of *Listeria monocytogenes* by Food Antimicrobials Applied Singly and in Combination. *Journal of Food Science*, *75*(9), M557–M563. <https://doi.org/10.1111/j.1750-3841.2010.01843.x>
- Brayner, R., Ferrari-Iliou, R., Brivois, N., Djediat, S., Benedetti, M. F., & Fiévet, F. (2006). Toxicological impact studies based on *Escherichia coli* bacteria in ultrafine ZnO nanoparticles colloidal medium. *Nano Letters*, *6*(4), 866–870. <https://doi.org/10.1021/nl052326h>
- Buzea, C., Pacheco, I. I., & Robbie, K. (2007). Nanomaterials and nanoparticles: Sources and toxicity. *Biointerphases*, *2*(4), MR17–MR71. <https://doi.org/10.1116/1.2815690>
- Chamjangali, M. A., & Boroumand, S. (2013). Synthesis of flower-like Ag-ZnO nanostructure and its application in the photodegradation of methyl orange. *Journal of the Brazilian Chemical Society*, *24*(8), 1329–1338. <https://doi.org/10.5935/0103-5053.20130168>
- Chandra, S., Rawat, D. S., & Bhatt, A. (2021). Phytochemistry and pharmacological activities of *saponaria officinalis* L.: A review. *Notulae Scientia Biologicae*, *13*(1), 1–13. <https://doi.org/10.15835/nsb13110809>
- Cheng, B., Shi, W., Russell-Tanner, J. M., Zhang, L., & Samulski, E. T. (2006). Synthesis of Variable-Aspect-Ratio, Single-Crystalline ZnO Nanostructures. *ChemInform*, *37*(17), 1208–1214. <https://doi.org/10.1002/chin.200617225>
- da Silva, E. C., de Moraes, M. O. S., Brito, W. R., Passos, R. R., Brambilla, R. F., da Costa, L. P., & Pocrifka, L. A. (2020). Synthesis of ZnO Nanoparticles by the Sol-Gel Protein Route: A Viable and Efficient Method for Photocatalytic Degradation of Methylene Blue and Ibuprofen. *Journal of the Brazilian Chemical Society*, *31*(8), 1648–1653. <https://doi.org/10.21577/0103-5053.20200050>
- Elumalai, K., & Velmurugan, S. (2015). Green synthesis, characterization and antimicrobial activities of zinc oxide nanoparticles from the leaf extract of *Azadirachta indica* (L.). *Applied Surface Science*, *345*, 329–336. <https://doi.org/10.1016/j.apsusc.2015.03.176>
- Endonova, G. B., Antsupova, T. P., Zhamsaranova, S. D., & Lygdenov, D. V. (2015). Study of flavonoid and antioxidant activity of *saponaria officinalis* L. that occurs in Buryatia. *Biosciences Biotechnology Research Asia*, *12*(3), 2017–2021. <https://doi.org/10.13005/bbra/1869>
- Gnanadesigan, M., Anand, M., Ravikumar, S., Maruthupandy, M., Syed Ali, M., Vijayakumar, V., & Kumaraguru, A. K. (2012). Antibacterial potential of biosynthesised silver nanoparticles using *Avicennia marina* mangrove plant. *Applied Nanoscience (Switzerland)*, *2*(2), 143–147. <https://doi.org/10.1007/s13204-011-0048-6>
- Guo, D., Xie, G., & Luo, J. (2014). Mechanical properties of nanoparticles: Basics and applications. *Journal of Physics D: Applied Physics*, *47*(1). <https://doi.org/10.1088/0022-3727/47/1/013001>
- Halbus, A. F., Horozov, T. S., & Paunov, V. N. (2020). Surface-Modified Zinc Oxide Nanoparticles for Antialgal and Antiyeast Applications. *ACS Applied Nano Materials*, *3*(1), 440–451. <https://doi.org/10.1021/acsnm.9b02045>
- Hassan, H. S., Elkady, M. F., El-Sayed, E. M., Hamed, A. M., Hussein, A. M., & Mahmoud, I. M. (2018). Synthesis and characterization of zinc oxide nanoparticles using green and chemical synthesis techniques for phenol decontamination. *International Journal of Nanoelectronics*

- and *Materials*, 11(2), 179–194.
- Huang, Z., Zheng, X., Yan, D., Yin, G., Liao, X., Kang, Y., ... Hao, B. (2008). Toxicological effect of ZnO nanoparticles based on bacteria. *Langmuir*, 24(8), 4140–4144. <https://doi.org/10.1021/la7035949>
- Jurado Gonzalez, P., & Sørensen, P. M. (2020). Characterization of saponin foam from *Saponaria officinalis* for food applications. *Food Hydrocolloids*, 101(August 2019). <https://doi.org/10.1016/j.foodhyd.2019.105541>
- Krishnan, D., & Pradeep, T. (2009). Precursor-controlled synthesis of hierarchical ZnO nanostructures, using oligoaniline-coated Au nanoparticle seeds. *Journal of Crystal Growth*, 311(15), 3889–3897. <https://doi.org/10.1016/j.jcrysgro.2009.06.019>
- Kucukkurt, I., Ince, S., Enginar, H., Eryavuz, A., Fidan, A. F., & Kargioglu, M. (2011). Protective effects of *Agrostemma githago* L. and *Saponaria officinalis* L. extracts against ionizing radiation-induced oxidative damage in rats. *Revue de Medecine Veterinaire*, 162(6), 289–296.
- Linsinger, T. P. J., Roebben, G., Solans, C., & Ramsch, R. (2011). Reference materials for measuring the size of nanoparticles. *TrAC - Trends in Analytical Chemistry*, 30(1), 18–27. <https://doi.org/10.1016/j.trac.2010.09.005>
- Luo, F., Yang, D., Chen, Z., Megharaj, M., & Naidu, R. (2016). One-step green synthesis of bimetallic Fe/Pd nanoparticles used to degrade Orange II. *Journal of Hazardous Materials*, 303, 145–153. <https://doi.org/10.1016/j.jhazmat.2015.10.034>
- Manzoor, U., Siddique, S., Ahmed, R., Noreen, Z., Bokhari, H., & Ahmad, I. (2016). Antibacterial, structural and optical characterization of mechano-chemically prepared ZnO nanoparticles. *PLoS ONE*, 11(5), 1–12. <https://doi.org/10.1371/journal.pone.0154704>
- Maruthupandy, M., Zuo, Y., Chen, J. S., Song, J. M., Niu, H. L., Mao, C. J., ... Shen, Y. H. (2017). Synthesis of metal oxide nanoparticles (CuO and ZnO NPs) via biological template and their optical sensor applications. *Applied Surface Science*, 397, 167–174. <https://doi.org/10.1016/j.apsusc.2016.11.118>
- Nayak, D., Ashe, S., Rauta, P. R., Kumari, M., & Nayak, B. (2016). Bark extract mediated green synthesis of silver nanoparticles: Evaluation of antimicrobial activity and antiproliferative response against osteosarcoma. *Materials Science and Engineering C*, 58, 44–52. <https://doi.org/10.1016/j.msec.2015.08.022>
- Padmavathy, N., & Vijayaraghavan, R. (2008). Enhanced bioactivity of ZnO nanoparticles - An antimicrobial study. *Science and Technology of Advanced Materials*, 9(3). <https://doi.org/10.1088/1468-6996/9/3/035004>
- Reddy, K. M., Feris, K., Bell, J., Wingett, D. G., Hanley, C., & Punnoose, A. (2007). Selective toxicity of zinc oxide nanoparticles to prokaryotic and eukaryotic systems. *Applied Physics Letters*, 90(21), 10–13. <https://doi.org/10.1063/1.2742324>
- Sadowska, B., Budzyńska, A., Wieckowska-Szakiel, M., Paszkiewicz, M., Stochmal, A., Moniuszko-Szajwaj, B., ... Różalska, B. (2014). New pharmacological properties of *Medicago sativa* and *Saponaria officinalis* saponin-rich fractions addressed to *Candida albicans*. *Journal of Medical Microbiology*, 63(PART 8), 1076–1086. <https://doi.org/10.1099/jmm.0.075291-0>
- Sawai, J., Shoji, S., Igarashi, H., Hashimoto, A., Kokugan, T., Shimizu, M., & Kojima, D. (1998). Factor in Zinc Oxide. *Journal of Fermentation and Bioengineering*, 86(5), 521–522.
- Selim, Y. A., Azb, M. A., Ragab, I., & H. M. Abd El-Azim, M. (2020). Green Synthesis of Zinc Oxide Nanoparticles Using Aqueous Extract of *Deverra tortuosa* and their Cytotoxic Activities. *Scientific Reports*, 10(1), 1–9. <https://doi.org/10.1038/s41598-020-60541-1>
- Sengul, M., Ercisli, S., Yildiz, H., Gungor, N., Kavaz, A., & Çetina, B. (2011). Antioxidant, antimicrobial activity and total phenolic content within the aerial parts of *artemisia absinthum*, *artemisia santonicum* and *saponaria officinalis*. *Iranian Journal of Pharmaceutical Research*, 10(1), 49–56. <https://doi.org/10.22037/ijpr.2010.877>
- Slobodianiuk, L., Budniak, L., Marchyshyn, S., Kostyshyn, L., & Zakharchuk, O. (2021). Analysis of carbohydrates in *Saponaria officinalis* L. using GC/MS method. *Pharmacia*, 68(2), 339–345. <https://doi.org/10.3897/PHARMACIA.68.E62691>
- Sutradhar, P., & Saha, M. (2015). Synthesis of zinc oxide nanoparticles using tea leaf extract and its application for solar cell. *Bulletin of Materials Science*, 38(3), 653–657. <https://doi.org/10.1007/s12034-015-0895-y>
- Tănase, M. A., Marinescu, M., Oancea, P., Răducan, A., Mihaescu, C. I., Alexandrescu, E., ... Cinteza, L. O. (2021). Antibacterial and photocatalytic properties of ZnO nanoparticles obtained from chemical versus *Saponaria officinalis* extract-mediated synthesis. *Molecules*, 26(7). <https://doi.org/10.3390/molecules26072072>
- Vijayakumar, S., Mahadevan, S., Arulmozhi, P., Sriram, S., & Praseetha, P. K. (2018). Green synthesis of zinc oxide nanoparticles using *Atalantia monophylla* leaf extracts: Characterization and antimicrobial analysis. *Materials Science in Semiconductor Processing*, 82(March), 39–45. <https://doi.org/10.1016/j.mssp.2018.03.017>
- Wahab, R., Kaushik, N. K., Verma, A. K., Mishra, A., Hwang, I. H., Yang, Y. B., ... Kim, Y. S. (2011). Fabrication and growth mechanism of ZnO nanostructures and their cytotoxic effect on human brain tumor U87, cervical cancer HeLa, and normal HEK cells. *Journal of Biological Inorganic Chemistry*, 16(3), 431–442. <https://doi.org/10.1007/s00775-010-0740-0>
- Xia, T., Kovoichich, M., Liong, M., Mädler, L., Gilbert, B., Shi, H., ... Nel, A. E. (2008). Comparison of the mechanism of toxicity of zinc oxide and cerium oxide nanoparticles based on dissolution and oxidative stress properties. *ACS Nano*, 2(10), 2121–2134. <https://doi.org/10.1021/nm800511k>
- Yuvakkumar, R., Suresh, J., Nathanael, A. J., Sundrarajan, M., & Hong, S. I. (2014). Novel green synthetic strategy to prepare ZnO nanocrystals using rambutan (*Nephelium lappaceum* L.) peel extract and its antibacterial applications. *Materials Science and Engineering C*, 41, 17–27. <https://doi.org/10.1016/j.msec.2014.04.025>
- Zarrindokht Emami-Karvani. (2012). Antibacterial activity of ZnO nanoparticle on Gram-positive and Gram-negative bacteria. *African Journal of Microbiology Research*, 5(18), 1368–1373. <https://doi.org/10.5897/ajmr10.159>